CHAPTER 3

Plasma Ionization: Glow Discharge and RF Spark Source

Glow Discharge Basics

1. Introduction: What Is a Glow Discharge, and What Is It Used For?

A glow discharge (GD) is a plasma, that is, a partially ionized gas consisting of electrons and positive (and sometimes negative) ions, as well as a large number of neutral species. It is created by applying a potential difference (of the order of 1 kV) between two electrodes that are inserted in a cell filled with a gas, or that form the cell walls. In analytical GDs, the gas is usually argon, and the gas pressure is typically in the range of 50–700 Pa.

In the absence of a potential difference, cosmic radiation would induce the emission of a few electrons from the electrodes, but these electrons are not able to sustain a discharge. However, when a potential difference is applied, the electrons are accelerated away from the cathode, and they give rise to ionization and excitation collisions with the argon gas atoms. The ionization collisions create argon ions and new electrons. The argon ions are accelerated toward the cathode, where they release new electrons (i.e., 'secondary electron emission'). The electrons can again give rise to ionization, creating new electrons and argon ions. In this way, a 'self-sustaining plasma' is created. Electron excitation of the argon atoms gives rise to atoms in excited levels, which will decay to lower levels by emission of radiation. The latter explains the characteristic name of the 'glow' discharge (e.g., it emits a blue glow in argon). These elementary processes are schematically represented in Fig. 1.

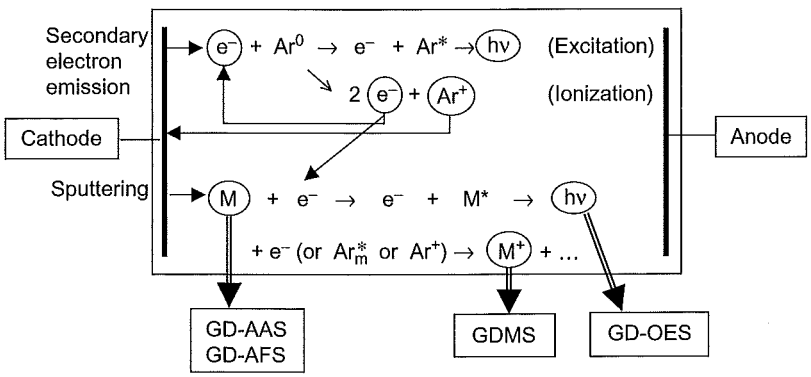

Figure 1
Schematic diagram of the basic processes in an analytical argon GD (i.e., electron impact excitation and ionization, secondary electron emission, and sputtering), as well as the analytical applications (GD-AAS, GD-AFS, GDMS and GD-OES). Ar^0, Ar^+, Ar^*, and Ar^*_m denote the Ar ground state atoms, Ar^+ ions, and Ar excited atoms in general and in the metastable levels, respectively. e^- and $h\nu$ symbolize the electrons and photons, respectively, and M, M^*, and M^+ stand for the sputtered (metal) atoms, excited atoms, and ions, respectively. Reproduced with permission from Jakubowski, N.; Bogaerts, A.; Hoffmann, V. Analytical Glow Discharges; Chapter 4. In: *Atomic Spectroscopy in Elemental Analysis*; Cullen, M., Ed.; Blackwell Publishing CRC Press, 2004; pp 91–156.

The use of the GD in analytical chemistry (see this chapter: *Glow Discharge Applications: Conductors and Semiconductors*; *Glow Discharge Applications: Radio Frequency Glow Discharges for Insulators*; *Glow Discharge Applications: Nuclear*) is based on a process called 'sputtering,' as is also illustrated in Fig. 1. The material to be analyzed is used as the cathode of the GD, which is bombarded by argon ions, accelerated by the electric field. These ions do not only release secondary electrons but also atoms of the cathode material, and this is called sputtering (see also Chapter 5 (this volume): *Sputtering and Ionization Basics*). The sputtered, analytically important atoms arrive in the plasma, where they undergo collisions. The ionization collisions (by electrons or other plasma species; see section 5.2 below) create ions of the cathode material, which can be measured in a mass spectrometer, thus giving rise to GDMS. The excitation collisions yield excited atoms, which release photons, characteristic of the elements present in the material to be analyzed. These photons can be detected with an optical emission spectrometer, giving rise to GD-OES. Moreover, the sputtered atoms can also directly be detected in the plasma with atomic absorption or fluorescence spectrometry (GD-AAS and GD-AFS). These analytical applications are also schematically represented in Fig. 1.

Besides in analytical chemistry, GDs are also used extensively in many other applications, such as for etching of surfaces or deposition of thin films, in the semiconductor industry, and for materials engineering, as lamps or lasers, in plasma display panels (TV screens), for biomedical applications (e.g., sterilization of materials), or for environmental purposes (e.g., the destruction of volatile compounds) (*1*). However, in this article, only analytical GD plasmas will be discussed. Most of the information presented here is based on the results of numerical modeling for GDs, developed by Bogaerts *et al.* (*2–5*), as well as on experimental verifications of this modeling work (*4,5*).

2. *Typical Operating Conditions and Electrical Operation Modes of a GD*

Analytical GDs, in the direct current (dc) mode, typically operate at a voltage of 500–1400 V, an electrical current of 1–100 mA, and an argon gas pressure of 50–700 Pa. The gas temperature ranges from room temperature till 1000 K. Typical current–voltage–pressure characteristics, as obtained from modeling calculations (and verified with experiments), are illustrated in Fig. 2. Often, GDs used as ion source for MS operate at lower pressure, gas temperature, and electrical current than GDs used for optical emission spectrometry (cf. curves with stars vs. curves with full circles in Fig. 2, respectively).

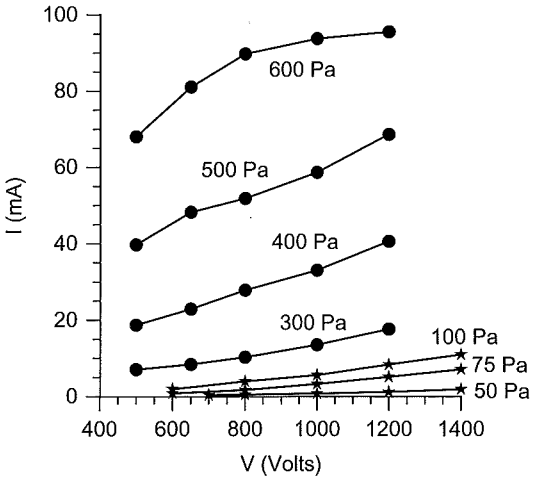

Figure 2
Electrical current as a function of voltage at different pressures, as obtained from numerical modeling, for a dc GD. The stars illustrate typical conditions of GDMS (VG9000 source), whereas the full circles represent typical GD-OES conditions (Grimm-type source). Reproduced with permission from Jakubowski, N.; Bogaerts, A.; Hoffmann, V. Analytical Glow Discharges; Chapter 4. In: *Atomic Spectroscopy in Elemental Analysis*; Cullen, M., Ed.; Blackwell Publishing CRC Press, 2004; pp 91–156.

However, this subdivision is rather artificial and mainly caused by instrumental considerations (e.g., pressure limitation when coupled to a mass spectrometer). Indeed, GDMS can also be operated at similar pressure as GD-OES (*6*).

Besides the dc mode, analytical GDs are more and more operated in radio frequency (rf) mode or pulsed mode. The typical operating conditions of an analytical rf GD are quite similar to a dc GD; however, the applied voltage and current vary as a function of time. Hence, the rf-powered electrode (which is constructed out of the material to be analyzed) acts alternately as cathode and anode. This makes the analysis of nonconducting materials possible, because the charge built up during positive ion bombardment will be neutralized by electron bombardment during part of the rf cycle (see also this chapter: *Glow Discharge Applications: Radio Frequency Glow Discharges for Insulators*). The rf is typically 13.56 MHz. Because of the large difference in size between rf-powered electrode (i.e., sample to be analyzed) and grounded electrode (i.e., cell walls), a large negative dc-bias voltage is typically developed in front of the rf-electrode, enabling sufficient ion bombardment and hence sputtering. This large dc-bias voltage makes the analytical rf discharge very similar to the dc GD, as far as plasma species densities and processes are concerned.

In the pulsed operation mode, the voltage and current are applied during short pulses (milli- or microsecond range). Because higher pulse voltages and currents (e.g., 2 kV, 1 A) can be applied for the same average power as in a dc GD, higher ionization and excitation rates can be obtained, yielding higher analyte signals, and hence lower detection limits than with a dc GD. Because analytical rf and pulsed GDs are not fundamentally different from dc GDs, the following sections focus on dc GDs. The differences between dc, rf, and pulsed GDs are discussed, for example, in refs. (*5*) and (*7*).

3. *Spatial Regions in the Analytical GD*

Although classical textbooks show a whole series of glowing and dark spaces in dc GDs (i.e., Aston dark space, cathode layer, cathode dark space (CDS), negative glow (NG), Faraday dark space, positive column, anode dark space (ADS), and anode glow) (*8*), the analytical GD can roughly be subdivided in three spatial regions (see Fig. 3, which is the result of modeling calculations at a pressure of 75 Pa, a voltage of 1000 V, and a current of 3 mA (*2,4*). These three regions are characterized by different behavior of the potential difference or electric field strength (Fig. 3b), light intensity (related to Fig. 3c), and charged species densities (Fig. 3d).

The potential difference applied between anode and cathode drops off completely in the first millimeters in front of the cathode, that is, in the region called 'cathode dark space.' Hence, this region is characterized by a strong negative electric field (Fig. 3b). The latter accelerates the electrons away from the cathode, and they traverse this region without many collisions (excitation, ionization, etc.). The name 'cathode dark space' originates from the low number of excitation collisions (Fig. 3c), and hence low de-excitation rate with emission of light. The CDS is characterized by a positive space charge; that is, the argon ion density is nearly constant and rather low, but the electron density is roughly zero (Fig. 3d), which explains the large potential drop.

After a few millimeters, the potential crosses zero and becomes slightly positive. This positive value (order of several volts) is nearly constant till the anode and gives rise to a very low electric field (see Fig. 3b). Hence, the electrons are not much accelerated, and they wander around, giving rise to many collisions in this region. The large number of excitation collisions (Fig. 3c), and the subsequent radiative decay, explains why this region is very bright. It is therefore called the 'negative glow' (NG). Ion and electron densities are rather high and nearly equal to each other (Fig. 3d), giving rise to more or less charge neutrality, which explains the nearly constant potential of Fig. 3b.

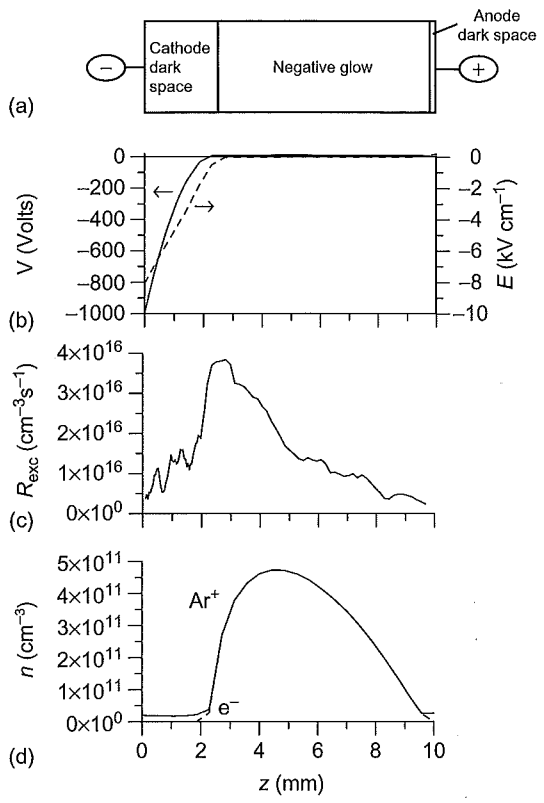

Figure 3
Schematic diagram of the different spatial regions in an analytical GD (a), and the corresponding potential and electric field distributions (b), electron excitation rate (c), and Ar^+ ion and electron density profiles (d), as obtained from numerical modeling, at 1000 V, 75 Pa, and 3 mA. Reproduced with permission from Jakubowski, N.; Bogaerts, A.; Hoffmann, V. Analytical Glow Discharges; Chapter 4. In: *Atomic Spectroscopy in Elemental Analysis*; Cullen, M., Ed.; Blackwell Publishing CRC Press, 2004; pp 91–156.

Close to the anode, the potential returns to zero, and the electric field is slightly positive (Fig. 3b). This so-called anode dark space is again characterized by a low and nearly constant positive ion density and a nearly zero electron density (Fig. 3d).

4. *Species Present in the Analytical GD*

Table 1 gives an overview of the most important species present in an analytical GD, as well as the range of their densities, calculated for the typical range of analytical GD conditions (see beginning of section 2) (*2–5*). The analytical GD is usually maintained in argon, and the *argon gas atoms* are the

Table 1
Overview of the most important plasma species and their densities, obtained from modeling calculations, in the typical range of analytical glow discharge conditions (see Fig. 2; i.e., voltage of 500–1400 V, pressure of 50–700 Pa, gas temperature of 300–1000 K, and electric current of 1–100 mA)

Species	Calculated range of densities (cm^{-3})
Argon gas atoms	10^{16}–10^{17}
Ar^+ ions	10^{11}–10^{14}
Electrons	10^{11}–10^{14}
Argon atoms in 4s metastable levels	10^{11}–10^{13}
Sputtered (Cu) atoms	10^{12}–10^{14}
Cu^+ ions	10^{9}–10^{12}

dominant plasma species, with typical densities in the order of 10^{16}–$10^{17}\,cm^{-3}$, in typical analytical discharge conditions.

When the argon gas flow is rather low, the gas atoms can be considered at thermal velocities, and the gas density will be more or less uniform, but somewhat depleted near the cathode as a result of gas heating. Indeed, gas heating is especially important near the cathode (*9*), and a higher gas temperature yields a lower density, for a fixed pressure, based on ideal gas law ($n = N/V = p/kT$). Figure 4 shows a typical calculated gas temperature profile, and the corresponding Ar gas atom density distribution, at 800 V, 500 Pa, and approximately 50 mA. Under these conditions, the gas temperature reaches values of approximately 700 K near the cathode, but drops to room temperature at approximately 1 cm from the cathode. Correspondingly, the Ar gas atom density is nearly constant (almost $10^{17}\,cm^{-3}$) from approximately 1 cm from the cathode till the end of the discharge (which can be several centimeters long), but it drops to approximately $4 \times 10^{16}\,cm^{-3}$ near the cathode. It should be mentioned that at lower pressure, voltage or current, the temperature does not rise to such a large extent, and the gas atom density remains more constant throughout the discharge.

When a considerable gas flow is applied to the GD, for instance, to increase the ion transport toward the mass spectrometer, there will be a convective flow throughout the discharge (*10*), which affects the gas density distribution. Figure 5 illustrates the Ar gas density profile, as calculated with a computational fluid dynamics (CFD) code, assuming a gas inlet flow rate of 100 sccm (*10*). The gas density is highest near the gas inlet, and lowest at the gas outlet, as expected. In the main part of the discharge cell, however, the gas density is fairly uniform, with values in the order of $4–5 \times 10^{16}\,cm^{-3}$. However, the effect of gas heating is not taken into account in this CFD code. Hence,

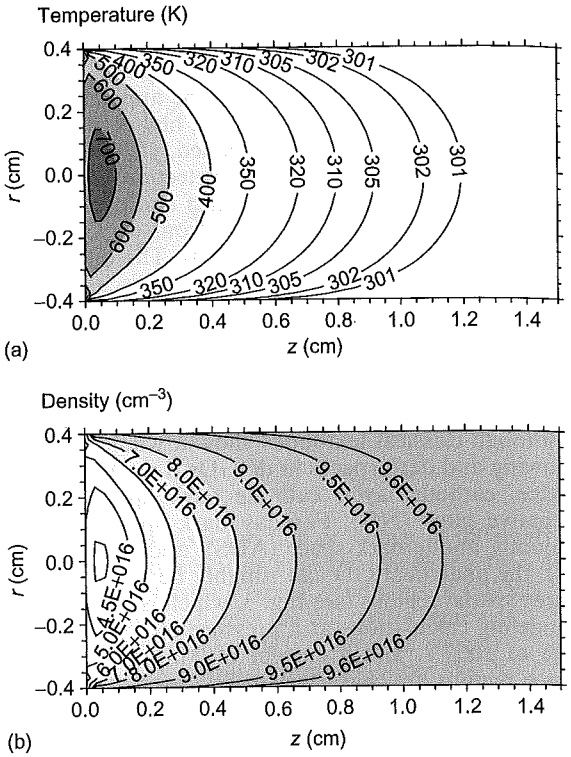

Figure 4
Calculated argon gas temperature distribution (a) and gas atom density distribution (b) (*9*), for a Grimm-type source, at 800 V, 500 Pa, and approximately 50 mA. Note that only the first 1.5 cm near the cathode of the Grimm-type cell is shown. Reproduced with permission from Jakubowski, N.; Bogaerts, A.; Hoffmann, V. Analytical Glow Discharges; Chapter 4. In: *Atomic Spectroscopy in Elemental Analysis*; Cullen, M., Ed.; Blackwell Publishing CRC Press, 2004; pp 91–156.

the real gas density distribution is probably a combination of Fig. 4b and Fig. 5.

Although most of the argon gas is in atomic form, a small fraction (order of 10^{-5}–10^{-3}) is ionized. Figure 6 shows the calculated *Ar^+ ion* density distribution, for the same conditions as in Fig. 4. The Ar^+ ion density is rather low in the CDS, and reaches a maximum at a few millimeters from the cathode. Note that the *electron* density is characterized by nearly the same profile, except that it is nearly zero in the CDS (see also Fig. 3). The Ar^+ ion and electron densities typically range from 10^{11} to $10^{14}\,cm^{-3}$, in typical analytical GD conditions, increasing with voltage, pressure, and current. The agreement is fairly good between calculated electron densities and experimental values (*3,11*).

The Ar^+ ions are usually the dominant ionic species in the GD plasma. The Ar^{2+} and Ar_2^+ ions have

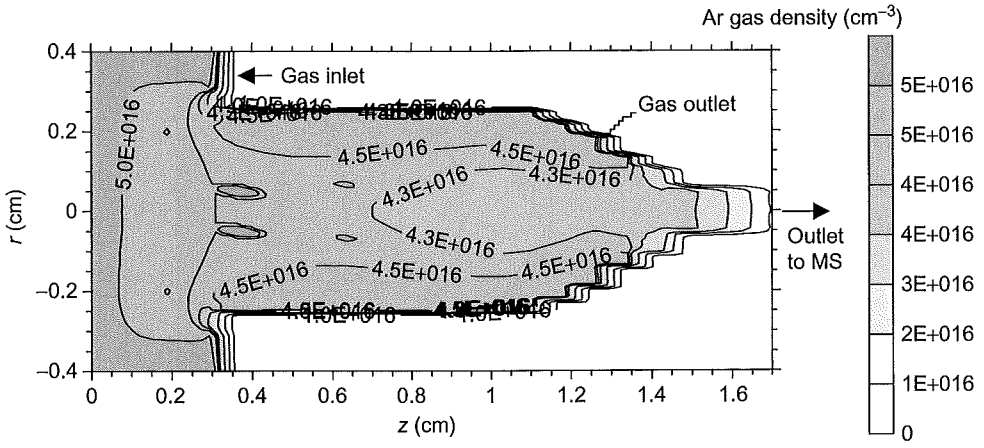

Figure 5
Calculated argon gas density distribution for a modified Grimm-type ion source for MS, with high gas flow rate (100 sccm). The positions of gas inlet and outlet are also indicated. The white areas denote the plasma boundaries (cell walls, see ref. *10*).

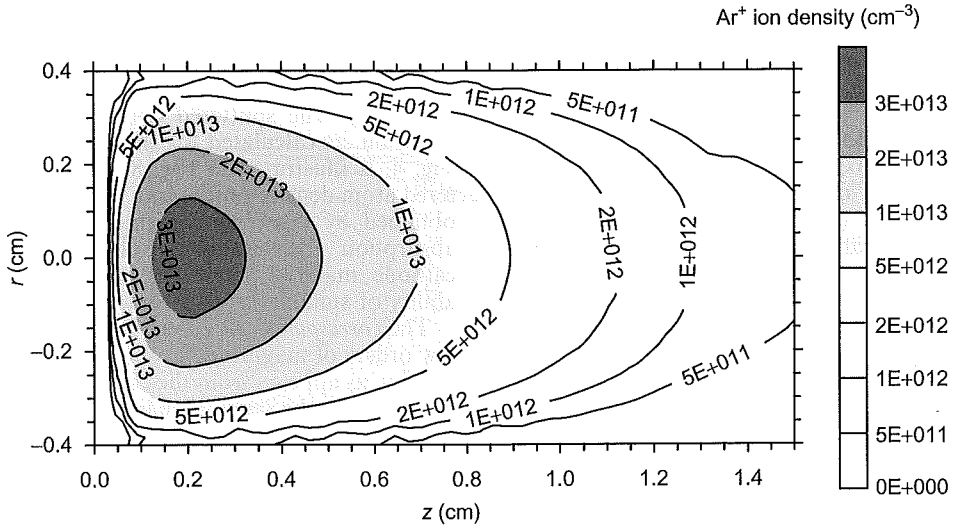

Figure 6
Calculated Ar^+ ion density distribution (*3*), for a Grimm-type source, at the same conditions as in Fig. 4. Reproduced with permission from Jakubowski, N.; Bogaerts, A.; Hoffmann, V. Analytical Glow Discharges; Chapter 4. In: *Atomic Spectroscopy in Elemental Analysis*; Cullen, M., Ed.; Blackwell Publishing CRC Press, 2004; pp 91–156.

typically much lower densities (e.g., 2 orders of magnitude lower than the Ar^+ ion density, as calculated in ref. *12*). When small traces of impurities are present in the argon gas, other ionic species can also be formed in the plasma. Modeling calculations show that when small amounts (few percentage) of H_2 are added to the argon gas, ArH^+ and H_3^+ ions are also present, with densities only 1 order of magnitude lower than the Ar^+ ion density (*13*).

Besides argon atoms and ions in the ground state, excited species are also present in the GD plasma. The most important are the *argon atoms in the two 4s metastable levels* (i.e., the lowest excited levels, at 11.55 and 11.72 eV, which cannot decay spontaneously to the ground state by emission of radiation). Indeed, the Ar metastable atoms play an important role in ionization of the sputtered atoms (Penning ionization; see later in text). Figure 7 illustrates the density

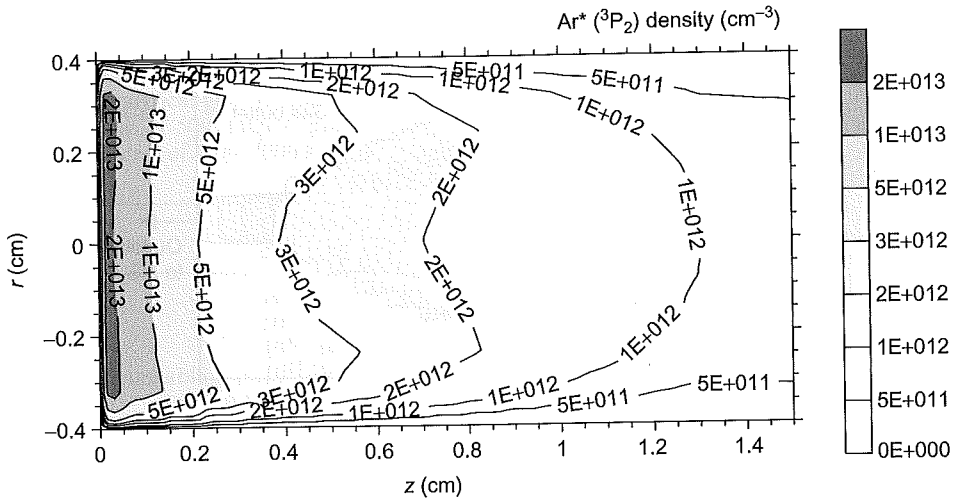

Figure 7
Calculated density distribution of the Ar* $^3P_2$ metastable level, for a Grimm-type source, at the same conditions as in Fig. 4. Reproduced with permission from Jakubowski, N.; Bogaerts, A.; Hoffmann, V. Analytical Glow Discharges; Chapter 4. In: *Atomic Spectroscopy in Elemental Analysis*; Cullen, M., Ed.; Blackwell Publishing CRC Press, 2004; pp 91–156.

distribution of the ($3p^5$ 4s) $^3P_2$ metastable level, calculated for the same conditions as in Fig. 4. The density reaches a maximum of $2 \times 10^{13}\,cm^{-3}$ adjacent to the cathode, and drops to values in the order of $10^{12}\,cm^{-3}$ farther in the discharge. This pronounced maximum near the cathode is attributed to production of this level by fast argon ion and atom excitation. Indeed, these processes are more important as a production mechanism than electron excitation, in typical analytical discharge conditions (*14*). The other metastable level, that is, the ($3p^5$ 4s) $^3P_0$ level, has a similar density profile, but is a factor of 2–5 lower (*14*).

Beside the two 4s metastable levels, there are also two other 4s levels (i.e., at 11.62 and 11.83 eV), which can decay radiatively to the ground state. However, this radiation is easily reabsorbed by the argon ground state atoms, because of their high density, so that the fraction of radiation that is not reabsorbed (so-called escape factor) is only in the order of 10^{-3}–10^{-4} for typical analytical GD conditions (*14*). Hence, the 4s *nonmetastable excited levels* (*also called resonant levels*) are also characterized by rather high densities, that is, comparable to the Ar 4s metastable levels adjacent to the cathode, but they drop more quickly as a function of distance from the cathode (*14*).

Besides argon species, there are also sputtered atoms and ions present in the GD plasma. The *sputtered atom ground state* density in the plasma is typically 3–5 orders of magnitude lower than the argon atom density, and it is nonuniformly distributed, with a maximum near the cathode, as a result of sputtering. The sputtered copper atom density distribution, as calculated for the same conditions as in Fig. 4, is illustrated in Fig. 8. This calculated sputtered atom density profile is in agreement with results obtained by laser-induced fluorescence and atomic absorption measurements, albeit for a different cathode material (tantalum; because of the availability of suitable laser lines) (*5*).

The *corresponding Cu^+ ion ground state* density is a few orders of magnitude lower than the copper atom density, as appears from the calculated density profile in Fig. 9, for the same discharge conditions. The Cu^+ ion density reaches a maximum at the same position as the Ar^+ ion density (i.e., in the beginning of the NG; see figure 6); this in fact applies to all ionic species. The ionization degree of copper was calculated in the range of 10^{-4}–10^{-2}, for typical analytical GD conditions, rising with voltage, pressure, and current. This is significantly higher than the ionization degree of argon (see earlier in this section). Indeed, the sputtered atoms are much more efficiently ionized in the GD plasma than the argon atoms, due to Penning ionization by argon metastable atoms and asymmetric charge transfer with argon ions, as explained in the next section.

5. *Most Important Collision Processes in the Plasma*

The GD plasma is a complicated gas environment, consisting of many different species (see section 4

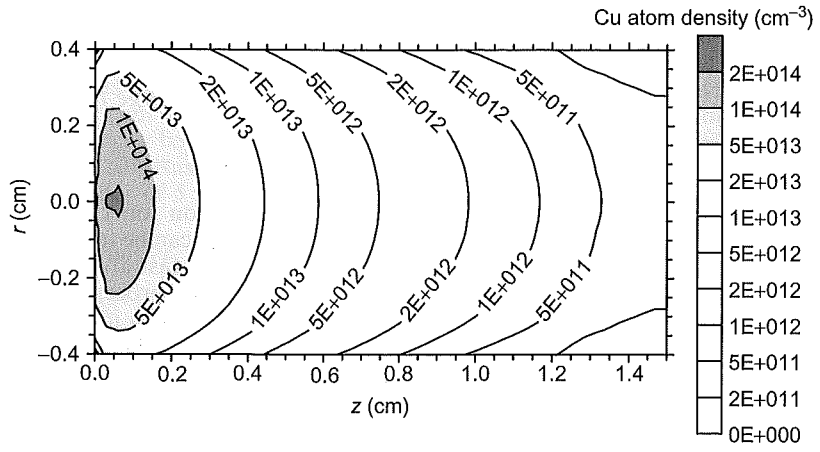

Figure 8
Calculated sputtered copper atom density distribution (*3*), for a Grimm-type source, at the same conditions as in Fig. 4. Reproduced with permission from Jakubowski, N.; Bogaerts, A.; Hoffmann, V. Analytical Glow Discharges; Chapter 4. In: *Atomic Spectroscopy in Elemental Analysis*; Cullen, M., Ed.; Blackwell Publishing CRC Press, 2004; pp 91–156.

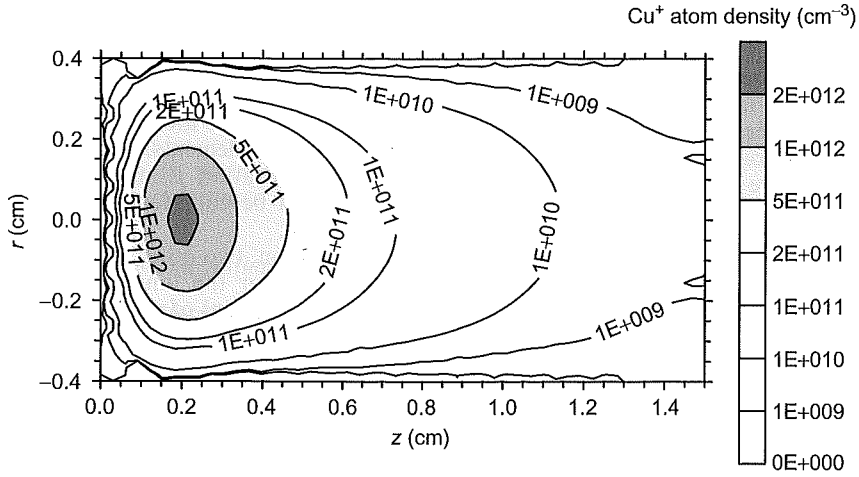

Figure 9
Calculated Cu^+ ion density distribution (*3*), for a Grimm-type source, at the same conditions as in Fig. 4. Reproduced with permission from Jakubowski, N.; Bogaerts, A.; Hoffmann, V. Analytical Glow Discharges; Chapter 4. In: *Atomic Spectroscopy in Elemental Analysis*; Cullen, M., Ed.; Blackwell Publishing CRC Press, 2004; pp 91–156.

above), which can all interact with each other. The most relevant and important processes for analytical GDs, that is, ionization (and recombination) and excitation (and de-excitation), are discussed here, along with the role of the various plasma species in these processes.

5.1 Ionization and Excitation of Argon Atoms

5.1.1 Electron ionization and excitation.

$$Ar^0 + e^- \rightarrow Ar^+ + 2e^-$$

$$Ar^0 + e^- \rightarrow Ar^* + e^-$$

Electron ionization is the essential process for sustaining the discharge, as the electrons formed in this way can again give rise to ionization, leading to electron multiplication (see Section 1). *Direct electron ionization* (i.e., from ground state argon atoms) is most important, although *two-step electron ionization* from argon atoms in the metastable levels can occur as well. Indeed, the minimum electron energy required for direct excitation is 15.76 eV (i.e., the ionization potential of argon), whereas the second process can already occur at electron energies above 4 eV. Nevertheless, the first process is much more important, because of the much higher argon ground state atom density compared to the argon metastable atom density.

The mechanism of *electron excitation* is the same as for ionization, but less energy is transferred, so that the electron is not ejected, but jumps only to a higher energy level within the atom. The minimum energy required is 11.55 eV (i.e., the energy of the lowest excited level).

5.1.2 Fast argon ion (Ar_f^+) and argon atom (Ar_f^0) ionization and excitation.

$$Ar^0 + Ar_f^+ \rightarrow Ar^+ + Ar_f^+ + e^-,\ Ar^0 + Ar_f^0 \rightarrow Ar^+ + Ar_f^0 + e^-$$
$$Ar^0 + Ar_f^+ \rightarrow Ar^* + Ar_f^+,\ Ar^0 + Ar_f^0 \rightarrow Ar^* + Ar_f^0$$

Argon ions and atoms can also cause ionization and excitation if their energy is sufficiently high (i.e., well above 100 eV). Such energetic (or also called 'fast') argon ions and atoms are only found near the cathode, where the ions have gained much energy from the electric field in the CDS. Hence, these processes are only significant adjacent to the cathode, and their importance increases with rising voltages. At a typical voltage of approximately 1 kV, fast argon ion and atom impact ionization and excitation are clearly not negligible. The importance of fast argon ion and atom impact excitation as population mechanisms for the Ar 4s excited levels was demonstrated in Fig. 7. Furthermore, although the relative contributions of fast argon ion and atom impact ionization to the total ionization of argon are calculated to be only in the order of 1–4% (for the Ar^+ ions) and 2–14% for the fast Ar atoms (*3*), inclusion of these processes in the modeling work is required to reproduce the experimental current–voltage characteristics.

5.1.3 Argon metastable atom collisions leading to the ionization of one of the atoms.

$$Ar_m^* + Ar_m^* \rightarrow Ar^+ + Ar^0 + e^-$$

When two argon metastable atoms collide with each other, they have together sufficient energy (two times 11.55 or 11.72 eV) to knock off one electron and hence to yield the ionization of one of the atoms. This process contributes, however, a few percentage at the most to the overall ionization in analytical GDs.

5.1.4 Symmetric charge transfer.

$$Ar_f^+ + Ar_s^0 \rightarrow Ar_f^0 + Ar_s^+$$

When a fast argon ion collides with a slow argon atom, an electron can be transferred from the atom to the ion, creating a fast argon atom and a slow argon ion. Although this process is not a real ionization mechanism, as no extra ion and electron are created, it is mentioned here, because it is of major importance in the GD. Indeed, this process is responsible for the creation of a large number of fast argon atoms, which play an important role for ionization and excitation of argon (see section 5.1.2 above) and especially for cathode sputtering (see section 6.2 below).

5.2 Ionization and Excitation of Sputtered (Analyte) Atoms

5.2.1 Electron ionization and excitation. In principle, the same processes that cause the ionization and excitation of argon atoms apply also to the ionization and excitation of analyte atoms. However, little is known about the above-mentioned processes for the analyte atoms. Only electron ionization data and some very limited electron excitation data are available from the literature, and only for some specific sputtered elements. Because the cross-section of electron ionization is similar for all elements, this process can be considered an unselective ionization mechanism.

In addition, two other collision types are of special importance for the ionization (and possibly simultaneous excitation) of analyte atoms, that is, Penning ionization by Ar metastable atoms and asymmetric charge transfer with Ar ions. Because these two processes are more important than electron ionization (i.e., the dominant ionization mechanism for argon), and because they are absent for argon, the sputtered atoms are more efficiently ionized in the GD than the argon atoms, leading to a higher ionization degree (see end of Section 4).

5.2.2 Penning ionization.

$$M^0 + Ar_m^* \rightarrow M^+ + Ar^0 + e^-$$

If a 4s metastable argon atom collides with an analyte atom, the energy of the metastable level (i.e., 11.55 or 11.72 eV) can be used to ionize the analyte atom if its ionization potential is lower than the metastable energy. Because this is the case for most atoms, Penning ionization is also more or less unselective, and it is expected to be the dominant ionization mechanism of

sputtered atoms, certainly in low-pressure GDs. The only elements that cannot be ionized by Penning ionization with argon metastable atoms are H, N, O, F, Cl, Br. Cross-section data of Penning ionization for all elements are scarce, but from the few data available in the literature, it can be deduced that the cross-sections between argon metastable atoms and analyte atoms are of the order of $5 \times 10^{15}\,cm^2$ (*15*).

5.2.3 Asymmetric charge transfer.

$$M^0 + Ar^+ \rightarrow (M^+)^* + Ar^0$$

Asymmetric charge transfer between an analyte atom and an argon ion (i.e., transfer of an electron from the atom to the ion) can occur if the energy difference between the argon ion (ground state or metastable level) and the energy levels of the resulting analyte ion is sufficiently small. Therefore, asymmetric charge transfer is a selective process.

Cross-section data are very difficult to find in the literature, at least for the typical (relatively low) ion energies in a GD, and between argon ions and typical analyte elements (for a discussion, see ref. *16*). However, the importance of this process in analytical GDs and in hollow cathode discharges has been experimentally demonstrated for several gas ion/analyte atom combinations, for example, Ar^+/Cu, Ne^+/Cu, He^+/Cu, Ne^+/Al, Ar^+/Fe, Ar^+/Ti, and Ne^+/Fe (*17,18*). For elements that have a good energy overlap with argon ions, the cross-section of asymmetric charge transfer is comparable to the cross-section of Penning ionization (*19*), and hence, both processes are then expected to be of comparable importance in the GD.

5.3 Positive Ion–Electron Recombination

Electron–ion recombination is the reverse process of ionization; that is, an electron coalesces with a positive ion to form a neutral atom. From the conservation laws of momentum and energy follows that a simple two-body coalescence is not allowed (*8*). However, some alternative recombination processes can in principle occur in rare gas discharges; that is,

- Three-body recombination ($A^+ + e^- + B \rightarrow A^0 + B$), where a third body (e.g., electron or atom) takes part in the collision process and takes away the excess energy, hence satisfying the conservation laws.
- Radiative recombination ($A^+ + e^- \rightarrow A^* + h\nu$), where the excess energy is carried away by a photon.
- Dissociative recombination ($AB^+ + e^- \rightarrow (AB)^* \rightarrow A^* + B$). In this case, a two-body recombination process is possible as the collision product can dissociate and the recombination energy is converted into kinetic and potential energy of the dissociation products.

However, based on rate constant data from the literature (*20*), and for typical electron and Ar^+ ion densities of the order of $10^{12}\,cm^{-3}$ (see Table 1), the Ar^+-electron recombination rate is estimated to be of the order of 10^{12}–$10^{13}\,cm^{-3}\,s^{-1}$. This is clearly lower than typical ionization rates (order of 10^{16}–$10^{17}\,cm^{-3}\,s^{-1}$; *2–4*). The rate constant of dissociative ionization (e.g., with Ar_2^+) ions is much higher (order of 10^{-7}–$10^{-6}\,cm^3\,s^{-1}$ (*20*)). Nevertheless, this process is also of minor importance, as Ar_2^+ ions are not considered to be dominant species in the GD plasma (see section 4 above). Hence, electron–ion recombination is expected to be negligible compared to ionization in analytical GDs, except in the afterglow of pulsed discharges, where the electrons have slowed down completely and electron–ion recombination is considered to be responsible for the so-called afterpeak in excited level populations and optical emission intensities (*21*). Finally, electron–ion recombination can occur also (and more easily) at the cell walls, where the wall acts as a third body, to take away the excess energy.

5.4 De-excitation

De-excitation is the inverse of excitation. Indeed, except for the metastable levels, the excited levels of the atoms and ions are only short-lived, and the electron configuration soon returns to the ground state in one or several transitions. Radiative decay (i.e., by emission of radiation) is the most probable de-excitation mechanism, and it is responsible for the light emitted by a 'glow' discharge.

6. *Processes Occurring at the Walls of a GD Cell*

When a particle collides at the walls of the GD cell, different phenomena may occur, depending on the kind of particle, namely, reflection, absorption, implantation, recombination, secondary electron emission, or sputtering. The latter two processes are of special importance for the analytical GD, and will therefore be discussed in more detail.

6.1 Secondary Electron Emission

Secondary electron emission is necessary to maintain the discharge, because new electrons are supplied to compensate for the electron losses at the walls. It can in principle occur at all walls, and can be caused by the bombardment of electrons, ions, neutrals, and photons.

Most important in analytical GDs is, however, ion- (and atom-) induced secondary electron emission at the cathode. For clean surfaces, the secondary electron emission coefficient γ (i.e., the number of electrons emitted per incident particle) is nearly independent of the ion or atom kinetic energy at energies below 500–1000 eV. It is typically in the order of 0.1 for positive

argon ions and nearly zero for neutral ground state argon atoms. At higher energies, γ starts to increase with the ion or atom kinetic energy (*8*). This suggests that secondary electron emission results from a constant potential energy component, and a kinetic energy component (similar for both) that only plays a role at sufficiently high energies. The potential energy component of the ions is of the order of the ionization potential, which seems amply sufficient for secondary electron emission. Neutral ground state atoms do not possess such a potential energy component, which explains why γ is negligible at energies below 500–1000 eV. However, metastable atoms do possess a potential energy (i.e., the energy of the excited metastable level); hence they will be able to give rise to secondary electron emission.

It should be noted that the ion- and atom-induced secondary electron emission coefficient is largely dependent on the surface conditions (crystal phase, contaminations). For contaminated (or 'gas-covered') surfaces, the secondary electron emission coefficients can vary over many orders of magnitude as a function of the bombarding energies (*22*). Moreover, the values characteristic of pure metals can differ significantly from the ones of alloys or nonconducting materials (*8*).

6.2 *Sputtering*

In contrast to secondary electron emission, sputtering is restricted to the cathode, as it requires sufficiently high bombarding energies. When energetic particles (i.e., gas ions or atoms and also ions of the cathode material) bombard the cathode surface, they can eject atoms lying at the surface, which is called sputtering. It is believed that the majority of the sputtered particles are neutral atoms. Ions can also be sputtered, but positive ions will immediately return back to the cathode, by the strong electric field in front of it. The energy of the sputtered atoms is of the order of a few electronvolts (*23*).

Figure 10 shows the relative contributions of fast argon ions, fast argon atoms, and cathode (copper) ions to the sputtering process, calculated for a range of different pressures and voltages. It appears that the fast argon atoms (Fig. 10a) play a dominant role in sputtering, at least in the low-pressure range or at low voltages. The reason is that a large number of fast argon atoms are created near the cathode, due to collisions of argon ions with argon gas atoms. Indeed, the flux of fast argon atoms bombarding the cathode is calculated to be typically 2 orders of magnitude higher than the flux of fast argon ions (*4*). The contribution of fast argon atoms is calculated to be on the order of 70% at low pressure and voltage, but this value drops to roughly 25% at the highest voltage and pressure investigated, due to the increasing role of sputtered copper ions (see below).

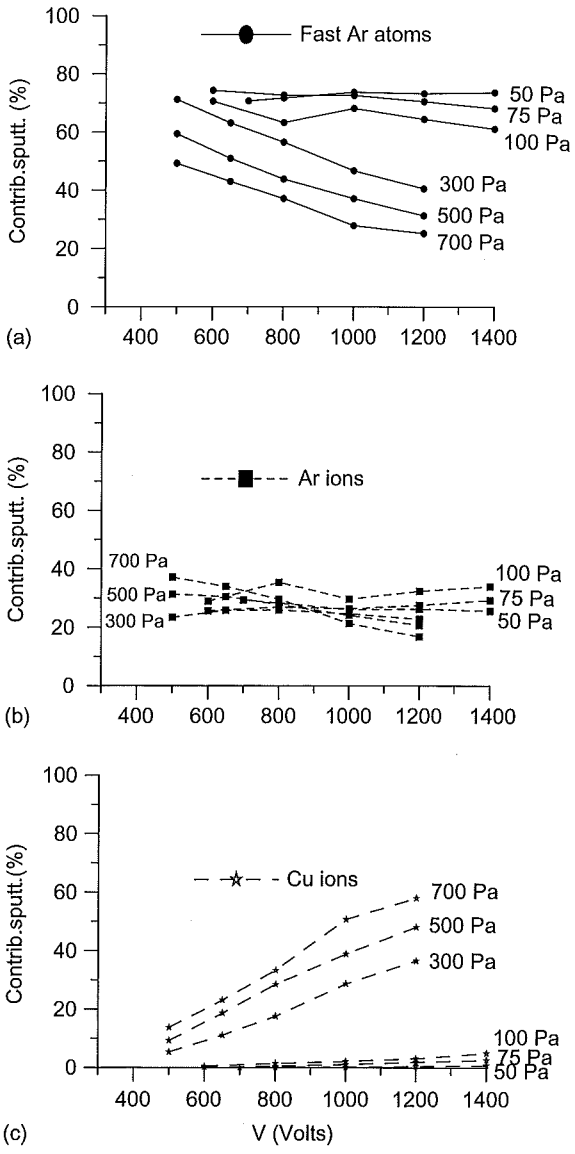

Figure 10
Calculated relative contributions to sputtering of the fast argon atoms (a), Ar^+ ions (b), and Cu^+ ions (c), as a function of voltage at different pressures, for typical VG9000 and Grimm-type conditions.

The contribution of argon ions to sputtering (Fig. 10b) is calculated to be on the order of 20–30%, at all pressures and voltages under study. Finally, the copper ions also play a nonnegligible role in sputtering, with a relative contribution of less than 1% at the lowest voltage and pressure investigated, and increasing till approximately 60% at the highest voltage and pressure under study (Fig. 10c). Indeed, although

the copper ions have a lower flux when bombarding the cathode (cf. the densities), they are characterized by much higher energies, and because the sputter yield increases with rising energy (see earlier in text), the role of copper ions (i.e., so-called self-sputtering) is not negligible, and appears to become even dominant at high voltage and pressure.

The sputter yield determines the number of sputtered atoms per incident particle. It is a complex function of the incident energy and the masses and atomic numbers of the bombarding particles and surface target (*24*). In general, the sputter yield increases less than linearly with the *mass of the incident particles*. Hence, the sputter yield does not reach a maximum when the masses of incident particles and surface target are close to each other (see examples in ref. *24*).

As far as the *energy of incident particles* is concerned, a threshold energy is required to give sputtering. Indeed, the atoms at the cathode surface must obtain sufficient energy to overcome their surface binding energy. Above this minimum energy, the sputter yield increases with the energy of the bombarding particles. It reaches a broad maximum at energies in the order of several kiloelectronvolts, after which it decreases again, as ion implantation becomes important (*8*).

The *cathode material* is also a determining factor for sputtering. The *cathode surface* has an influence on the sputter yield; for example, the sputter yield is decreased by surface contaminations, or by the formation of oxide layers or adsorbed gas layers on the cathode surface. As far as the *kind of cathode material* is concerned, in general, the sputter yield increases with the atomic number of the cathode material, within each row of the periodic table. However, the sputter yields of different elements seldom differ more than by 1 order of magnitude between each other, as opposed to the rates of evaporation, which differ by several orders of magnitude (*25*). Owing to these rather uniform sputter yields, the GD is relatively free from matrix effects, which has allowed GDMS to be ideally suited for selected applications, as will be discussed in this chapter: *Glow Discharge Applications: Conductors and Semiconductors*; *Glow Discharge Applications: Radio Frequency Glow Discharges for Insulators*; *Glow Discharge Applications: Nuclear*).

Bibliography

(*1*) Bogaerts, A.; Neyts, E.; Gijbels, R.; van der Mullen, J. Gas Discharge Plasmas and Their Applications. *Spectrochim. Acta Part B* **2002**, *57*, 609–658.

(*2*) Bogaerts, A.; Gijbels, R. Modeling of Glow Discharges: What Can We Learn from It? *Anal. Chem.* **1997**, *69*, 719A–727A.

(*3*) Bogaerts, A.; Gijbels, R. Comprehensive Description of a Grimm-Type Glow Discharge Source Used for Optical Emission Spectrometry: A Mathematical Simulation. *Spectrochim. Acta Part B* **1998**, *53*, 437–462.

(*4*) Bogaerts, A.; Gijbels, R. Modeling of Argon Direct Current Glow Discharges and Comparison with Experiment: How Good Is the Agreement? *J. Anal. At. Spectrom.* **1998**, *13*, 945–953.

(*5*) Bogaerts, A. Plasma Diagnostics and Numerical Simulations: Insight into the Heart of Analytical Glow Discharges. *J. Anal. At. Spectrom.* **2007**, *22*, 13–40.

(*6*) Jakubowski, N.; Feldmann, I.; Stüwer, D. Grimm-Type Glow Discharge Ion Source for Operation with a High Resolution Inductively Coupled Plasma-Mass Spectrometry Instrument. *J. Anal. At. Spectrom.* **1997**, *12*, 151–157.

(*7*) Bogaerts, A.; Gijbels, R. Similarities and Differences between Direct Current and Radio-Frequency Glow Discharges: A Mathematical Simulation. *J. Anal. At. Spectrom.* **2000**, *15*, 1191–1201.

(*8*) Chapman, B. *Glow Discharge Processes*; Wiley: New York, 1980.

(*9*) Bogaerts, A.; Gijbels, R.; Serikov, V. V. Calculation of Gas Heating in Direct Current Argon Glow Discharges. *J. Appl. Phys.* **2000**, *87*, 8334–8344.

(*10*) Bogaerts, A.; Okhrimovskyy, A.; Gijbels, R. Calculation of the Gas Flow and Its Effect on the Plasma Characteristics for a Modified Grimm-Type Glow Discharge Cell. *J. Anal. At. Spectrom.* **2002**, *17*, 1076–1082.

(*11*) Bogaerts, A.; Gijbels, R.; Gamez, G.; Hieftje, G. M. Fundamental Studies on a Planar-Cathode Direct Current Glow Discharge: Part II. Numerical Modeling and Comparison with Laser Scattering Experiments. *Spectrochim. Acta Part B* **2004**, *59*, 449–460.

(*12*) Bogaerts, A.; Gijbels, R. Role of Ar^{2+} and Ar_2^+ Ions in a Direct Current Glow Discharge: A Numerical Description. *J. Appl. Phys.* **1999**, *86*, 4124–4133.

(*13*) Bogaerts, A. Computer Simulations of Argon-Hydrogen Grimm-Type Glow Discharges. *J. Anal. At. Spectrom.* **2008**, *23*, 1476–1486.

(*14*) Bogaerts, A.; Gijbels, R.; Vlcek, J. Collisional-Radiative Model for an Argon Glow Discharge. *J. Appl. Phys.* **1998**, *84*, 121–136.

(*15*) Riseberg, L. A.; Parks, W. F.; Schearer, L. D. Penning Ionization of Zn and Cd by Noble-Gas Metastable Atoms. *Phys. Rev. A* **1973**, *8*, 1962–1968.

(*16*) Bogaerts, A.; Gijbels, R. Relative Sensitivity Factors in Glow Discharge Mass Spectrometry: The Role of Charge Transfer Ionization. *J. Anal. At. Spectrom.* **1996**, *11*, 841–847.

(*17*) Steers, E. B. M.; Fielding, R. J. Charge Transfer Excitation Processes in the Grimm Lamp. *J. Anal. At. Spectrom.* **1987**, *2*, 239–244.

(*18*) Farnsworth, P. B.; Walters, J. P. Excitation Processes in an rf Boosted, Pulsed Hollow Cathode Lamp. *Spectrochim. Acta Part B* **1982**, *37*, 773–788.

(*19*) Baltayan, P.; Pebay-Peyroula, J. C.; Sadeghi, N. Excitation of Zn^+* Levels in Penning and Charge Transfer Reactions of He* and He^+ with Zn. *J. Phys. B: At. Mol. Phys.* **1986**, *19*, 2695–2702.

(*20*) Biondi, M. A. Studies of the Mechanism of Electron-Ion Recombination. *Phys. Rev.* **1963**, *129*, 1181–1188.

(*21*) Jackson, G. P.; Lewis, C. L.; Doorn, S. K.; Majidi, V.; King, F. L. Spectral, Spatial and Temporal Characterization of a Millisecond Pulsed Glow Discharge: Metastable Argon Atom Production. *Spectrochim. Acta Part B* **2001**, *56*, 2449–2464.

(*22*) Phelps, A. V.; Petrovic, Z. L.j. Cold Cathode Discharges and Breakdown in Argon: Surface and Gas Phase

Production of Secondary Electrons. *Plasma Sources Sci. Technol.* **1999**, *8*, R21–R44.
(*23*) Stuart, R. V.; Wehner, G. K. Energy Distribution of Sputtered Cu Atoms. *J. Appl. Phys.* **1964**, *35*, 1819–1824.
(*24*) Matsunami, N.; Yamamura, Y.; Itikawa, Y., *et al.* Energy Dependence of the Ion-Induced Sputtering Yields of Monoatomic Solids. *Atom. Data Nucl. Data Tables* **1984**, *31*, 1–80.
(*25*) Harrison, W. W.; Bentz, B. L. Glow Discharge Mass Spectrometry. *Prog. Anal. Spectrosc.* **1988**, *11*, 53–110.

Annemie Bogaerts
University of Antwerp, Wilrijk-Antwerp, Belgium